Bioresource Technology 107 (2012) 419–428

Contents lists available at SciVerse ScienceDirect

Bioresource Technology

journal homepage: www.elsevier.com/locate/biortech

Impact of pyrolysis temperature and manure source on physicochemical characteristics of biochar

Keri B. Cantrell [a,*], Patrick G. Hunt [a], Minori Uchimiya [b], Jeffrey M. Novak [a], Kyoung S. Ro [a]

[a] USDA-ARS Coastal Plains Soil, Water & Plant Research Center, 2611 West Lucas Street, Florence, SC 29501, USA
[b] USDA-ARS Southern Regional Research Center, 1100 Robert E. Lee Boulevard, New Orleans, LA 70124, USA

ARTICLE INFO

Article history:
Received 1 July 2011
Received in revised form 21 November 2011
Accepted 23 November 2011
Available online 1 December 2011

Keywords:
Bioenergy
Black carbon
Plant nutrients
FTIR
Thermochemical conversion

ABSTRACT

While pyrolysis of livestock manures generates nutrient-rich biochars with potential agronomic uses, studies are needed to clarify biochar properties across manure varieties under similar controlled conditions. This paper reports selected physicochemical results for five manure-based biochars pyrolyzed at 350 and 700 °C: swine separated-solids; paved-feedlot manure; dairy manure; poultry litter; and turkey litter. Elemental and FTIR analyses of these alkaline biochars demonstrated variations and similarities in physicochemical characteristics. The FTIR spectra were similar for (1) turkey and poultry and (2) feedlot and dairy, but were distinct for swine biochars. Dairy biochars contained the greatest volatile matter, C, and energy content and lowest ash, N, and S contents. Swine biochars had the greatest P, N, and S contents alongside the lowest pH and EC values. Poultry litter biochars exhibited the greatest EC values. With the greatest ash contents, turkey litter biochars had the greatest biochar mass recoveries, whereas feedlot biochars demonstrated the lowest.

Published by Elsevier Ltd.

1. Introduction

Utilization of livestock manures as feedstocks for thermochemical conversion technologies has advantages of high temperature elimination of pathogens, drastically reducing waste stream volume, extracting useful energy from a livestock operation and the production of value-added products (Cantrell et al., 2008; Ro et al., 2010). Pyrolysis is the major anaerobic thermochemical conversion process leading to three product phases: noncondensable gas, condensable vapors; liquids (bio-oil and tars); and solid (char or ash). For targeting char production, slow pyrolysis is a technique that uses temperature ranges of 350–700 °C, slow heating rates of 1–100 °C s^{-1}, and long residence times (minutes–hours) (Spokas et al., 2011). When this char product is applied to soils with the intent to sequester carbon and maintain or improve soil fertility, it is commonly termed a biochar (Lehmann and Joseph, 2009; Spokas et al., 2011).

Biochars have been generated from a range of agricultural and organic materials (Spokas et al., 2011). Feedstock characteristics and pyrolysis conditions (e.g., maximum exposure temperature) affect the biochars' physical and chemical characteristics (Antal and Grønli, 2003; Gaskin et al., 2008; Novak et al., 2009; Singh et al., 2010). Plant-derived biochars (e.g., woody biomass and grasses) often have a low nutrient content. This low nutrient content is in part due to pyrolytic nitrogen losses (Sheth and Bagchi, 2005) and the low initial ash content of the feedstock as well as ash composition (often high in SiO_2 and CaO that are of lower nutrient values) (Bourke et al., 2007). With low nitrogen, phosphorous, and potassium contents, these plant-based biochars are disadvantageous when compared to traditional fertilizers for supplying crop nutrients. Conversely, manures are nutrient-rich materials; it correspondingly follows that pyrolysis of manures would produce a nutrient-rich biochar.

While there are an increasing number of papers reporting on the physical and chemical characteristics of biochar for use as soil amendments (e.g., Novak et al., 2009; Spokas et al., 2011) and soil contaminant remediation (e.g., Cao and Harris, 2010; Uchimiya et al., 2010), literature is limited on biochar characteristics derived from the wide selection of livestock animal manures and their structural diversity due to differences in pyrolytic temperature. Reported results have predominately pertained to poultry (broiler) litter biochar (e.g., Gaskin et al., 2008; Novak et al., 2009; Singh et al., 2010; Uchimiya et al., 2010). Other elemental and structural characterizations have been reported for swine and dairy (cow) manure-based biochars (e.g., Cantrell and Martin, 2011; Cao and Harris, 2010, 2011; Singh et al., 2010). Even though these studies have shown existence of both elemental and structural dissimilarities, the biochars were not produced under similar pyrolytic conditions. As such, there is a possibility that biochar property differences may be due to an array of production conditions. To more fully clarify biochar properties between different manure

* Corresponding author. Tel.: +1 843 669 5203x113; fax: +1 843 669 6970.
E-mail address: keri.cantrell@ars.usda.gov (K.B. Cantrell).

0960-8524/$ - see front matter Published by Elsevier Ltd.
doi:10.1016/j.biortech.2011.11.084

feedstocks under more controlled conditions, we present selected physicochemical and thermodynamical characteristics of 10 manure-based biochar – five varieties created under two temperature regimes.

2. Materials

2.1. Biomass

2.1.1. Dairy manure

Dairy manure samples (MD) were obtained from a 60-head milking facility in Harford County, MD. The dairy manure was collected within the milking parlor in a holding area. This parlor was a double 6 parabone that milked 12 cows at a time; the samples were collected across three milking replications. Cow rations consisted of a mixture of corn silage, alfalfa hay (as silage), corn grain, and a protein concentrate. The "as received" moisture content was determined to be 86.5 ± 0.4 wt.%.

2.1.2. Feedlot manure

Feedlot manure (FL) was obtained from a commercial deep-bedded facility in Sioux County, IA that was equipped with concrete floors in pens and barns. Within these facilities, shredded corn stalks were used as bedding material, and the pens were typically cleaned and re-bedded one–two times per week. The removed manure and bedding material was either stockpiled temporarily or applied directly to cropland. The "as received" moisture was determined to be 77.9 ± 0.5 wt.%.

2.1.3. Poultry litter

Poultry litter (PL) was collected from the top 5–7.5 cm depth along two transects longitudinally at 10 locations in a commercial poultry house in Orangeburg County, SC. This facility used soft wood shavings as bedding material. At the time of sampling, the house was empty of birds, but the bedding received excrement from between the 8 and 9 flocks that were raised for 5 weeks (8.5 flocks per year). Thus, the bedding was approximately 12 months old. The litter had an "as received" moisture of 23.7 ± 2.1 wt.%.

2.1.4. Separated swine solids

Separated swine solids (SW) were obtained from a polyacrylamide (PAM) polymer injected, solid–liquid separation system as part of a larger, three process waste treatment system on a 5600-head finishing swine operation in Sampson County, NC. The PAM separation system was separating a homogenized mixture of one week-old flushed swine manure and phosphate precipitate sludge stream. The "as received" moisture content was determined to be 78.5 ± 0.5 wt.%.

2.1.5. Turkey litter

Turkey litter (TL) used for this experiment was collected from a 7500 bird house in Lancaster County, SC. At the time of sampling, the house was on its second consecutive flock (3.5 flocks per year). The house was cleaned once a year with soft wood shavings serving as the bedding material. Approximately 75 L of litter was collected along the center transect of the house. The "as received" moisture content was calculated to be 26.1 ± 1.3%.

2.1.6. Preparation

Upon receipt, the MD and FL samples underwent initial convection drying at 60 °C. The SW samples underwent solar drying in a greenhouse. All initially dried MD, FL, and, SW samples, along with the PL and TL, were ground using a Wiley Mill equipped with a 2-mm screen. Sample grinding of all feedstocks was followed by overnight oven drying at 105 °C. The moisture content of ground material just prior to pyrolysis ("as pyrolyzed") ranged between 0.31% and 6.49%.

2.2. Pyrolysis system and process

Triplicate pyrolytic runs were performed at two temperatures – 350 and 700 °C. For each run, between 0.5 and 1.5 kg of prepared material was loaded onto a stainless steel tray and placed into a Lindburg electric box furnace equipped with a gas tight retort (Model 51662; Lindburg/MPH, Riverside, MI). The control scheme of this system was modified to that of a stochastic state-space regulator. In this scheme, temperature control was based on four input temperatures allowing for accurate control of pyrolytic exposure temperature. Details of this system and the control system can be found elsewhere (Cantrell and Martin, 2011).

Samples were pyrolyzed under the following temperature schedule: 60 min equilibration hold at 200 °C; ramp to desired pyrolytic temperature within 60 min (2.5 °C min^{-1} for 350 °C runs; 8.33 °C min^{-1} for 700 °C runs); 120 min equilibration hold at desired temperature; 4.25 °C min^{-1} cool down to 100 °C. During the 200 °C hold, the retort was purged using an industrial-grade N_2 gas flow at 15 L min^{-1}; the N_2 flow for the remaining operation was set to 1 L min^{-1} (equivalent to 0.6 and 0.04 retort chamber exchanges per min, respectively) to maintain anoxic conditions. After charring, the samples remained in an inert atmosphere but were allowed to cool to room temperature for subsequent removal from the retort. They were then homogeneously subsampled for analyzes.

2.3. Feedstock and biochar analyzes

2.3.1. Physical, chemical, and energetic properties

Both feedstock and biochar subsamples underwent the following analyzes: pH, electrical conductivity (EC), surface area, ultimate, proximate, energy content, and plant relevant minerals and metals. Results were reported for triplicate feedstock subsamples and an average value for the triplicate pyrolytic runs.

The pH and EC of the feedstock manures and biochars were measured in a 1% (w v^{-1}) suspension in deionized water prepared by shaking at 100 rpm for 2 h. The BET (Brunauer–Emmett–Teller) surface areas were measured via N_2 adsorption multilayer theory using a Nova 2200e surface area analyzer (Quantachrome, Boynton Beach, FL). The analysis was performed by Hazen Research, Inc. (Golden, CO) following ASTM D 3176 (CHNS) standard method (ASTM, 2006). The oxygen contents (O) for the feedstock and biochar subsamples were directly measured by dry combustion using a Perkin–Elmer 2400 Series II CHNS/O analyzer (Perkin–Elmer, Shelton, CT). These results were used to calculate atomic H/C, O/C, and (O + N)/C ratios to evaluate relationships between pyrolysis temperature and the relative degree of aromaticity (H/C ratio) and polarity (O/C and (O + N)/C ratios) of each biochar (Chen et al., 2008). For the proximate analysis, the ash content at 600 °C was determined by Hazen Research, Inc.; the volatile matter (VM) was determined using a thermogravimetric analyzer (TGA/DSC1; Mettler Toledo International Inc., Columbus, OH) following a recommended method in Cantrell and Martin (2011); and fixed carbon content was determined (following ASTM D 3172) as the difference between 100% and the additive of VM and ash (ASTM, 2006). The energy content or higher heating value (HHV) was determined using an isoperibol calorimeter (AC500; Leco Corp., St. Joseph, MI) following ASTM D 5865 standard method and corrected for N and S content before conversion to a dry basis as well as a dry ash-free basis (ASTM, 2006). Mineral and metal analyzes were performed for Al, As, Cd, Ca, Cr, Cu, Fe, K, Mg, Mn, Mo, Na, Ni, P, Pb, and Zn. These analyzes were performed by the Agricultural Service Laboratory at Clemson University (Clemson,

SC) using wet acid digestion (conc. HNO_3 + 30% H_2O_2) and quantified using inductive coupled plasma atomic emission spectroscopy (ICP-AES). This laboratory also analyzed samples for NO_3–N and NH_4–N, and soluble P concentrations using standard manure methods.

2.3.2. ATR-FTIR analysis

Further structural analysis was performed using Fourier transform infrared spectroscopy (FTIR) using a Bruker Vertex 70 spectrometer (Bruker Optics, Billerica, MA). This instrument was fitted with a MIRacle attenuated total reflectance (ATR) accessory (Pike Technologies, Madison, WI) and with a diamond crystal plate. The spectra were obtained at 8 cm^{-1} resolution from 650 to 4500 cm^{-1} using a combined 128 scans. All feedstock and biochar samples were analyzed without pretreatments.

The FTIR spectral peak assignments were interpreted based on characteristic vibrations for wood and grass biochars (Keiluweit et al., 2010), dairy manure (Calderón et al., 2006), dairy manure biochars (Cao and Harris, 2010), bio-oil obtained from fast pyrolysis of manures (Das et al., 2009; Xiu et al., 2010), natural organic matter (Wen et al., 2007), and bacterial surfaces (Jiang et al., 2004).

2.4. Recovery yields

Four recovery yields were determined for each pyrolytic run and were expressed on a C, ash, biochar weight basis and also a biochar energy basis. Biochar recovery (R_{BC}) was the percentage ratio of biochar mass to feedstock mass (m_B/m_F). On a dry, ash-free basis, the biochar recovery (R_{BCdaf}) was dependent on the feedstock and biochar ash contents (A_F and A_B; Eq. (1)) (Demirbaş, 2004). The C recovery (R_C) was calculated as the product of R_{BC} and ratio of biochar C content to feedstock C content. The ash and biochar energy recoveries were calculated similarly,

$$R_{BCdaf} = 100 \cdot \frac{A_F/A_B - A_F/100}{1 - A_F/100} \quad (1)$$

2.5. Statistical analyzes

When required, data were analyzed by Proc GLIMMIX (General Linear Mixed Model) in Version 9.2 of Statistical Analysis System (SAS Institute Inc., Cary, NC). Significant differences between treatments were based on pyrolytic temperature, feedstock type, or their interactions using an *F*-test (p-value < 0.05). Any tested correlations were identified using Proc CORR and p-values less than 0.05 were used for the Pearson's correlation test.

3. Results and discussion

3.1. Physical characteristics

Our results conform to well known progressions (Antal and Grønli, 2003; Bourke et al., 2007; Keiluweit et al., 2010) where more VM was removed with increasing temperature resulting in a stable, fixed carbon (Tables 1 and 2). Comparing the raw feedstocks and biochars within a pyrolysis temperature treatment, the VM contents had some differences and some similarities (Tables 1 and 2). The MD feedstock with the greatest VM generated biochars with the greatest VM content. On the other hand, SW feedstock produced a 700 °C biochar with the lowest VM content (Table 2). The other feedstocks and biochars were considered to be statistically similar.

Compared to their feedstocks, there were one to three fold increases in the biochar ash content. All ash contents were significantly different with values ranging from 24.2 ± 0.5 to 34.8 ± 0.1 wt.%$_{db}$ among the 350 °C biochars and 39.5 ± 1.6–52.9 ± 0.5 wt.%$_{db}$ for the 700 °C biochars (Tables 1 and 2). Similarly, the fixed carbon content increased 3–6 times compared to the feedstock (Tables 1 and 2). All manure-based biochars produced at 350 °C had statistically similar fixed carbon contents with an average of 24.2 ± 2.0 wt.%$_{db}$ except for SW (Tables 1 and 2). The SW 350 °C biochar had the lowest fixed carbon value of 17.7 ± 1.2 wt.%$_{db}$. At 700 °C, pyrolysis of TL feedstock produced biochar with the lowest concentration of fixed carbon (29.2 ± 3.8 wt.%$_{db}$); this was statistically similar to SW 700 °C biochar FC at 33.8 ± 0.5 wt.%$_{db}$ (Tables 1 and 2). In comparison, this was 20% lower than the other manure-based biochars with an average value of 34.8 ± 1.3 wt.%$_{db}$. From a carbon sequestration perspective, SW was the least suited among the manures to preserve carbon at low pyrolytic temperatures along with TL at high pyrolytic temperatures.

Pyrolyzing all of the raw feedstocks increased their pH and produced alkaline biochars (Tables 1 and 2). The heightened pH was related to pyrolysis temperature, with the 700 °C biochars being more alkaline than the 350 °C biochars. Contrastingly, the increase in alkalinity with temperature was not observed for cow manure biochars at 400 and 550 °C; they maintained a pH range of 8.9–9.0 (Singh et al., 2010). This is different from the current study, where both bovine varieties had the greatest pH among the 350 °C manure chars, 9.2. Both MD and FL pH continued to increase at 700 °C in excess of 9.9. The SW biochars were consistently lower in pH (than the other manure biochars) at 8.4 and 9.5, respectively for 350 and 700 °C. With alkaline pH-values as high as 10.3 for the PL and FL 700 °C biochars, these manure-based biochar additions to soils have been reported to have negative consequences on the soil chemistry of low-buffer capacity sandy soils (Novak et al., 2009). As such, their impact could be mediated through overall soil application rates.

It was also appropriate that the EC values of the biochars should be characterized to avoid creating unwanted salt effects in soils, especially at high biochar application rates (3–30 tones/ha; Lehmann and Joseph, 2009). Biochar EC values varied from 194 to 2217 μS cm^{-1} (Table 2). Biochars produced from PL had the greatest EC among all examined varieties. This was not surprising considering that PL is typically high in EC-influencing elements from incomplete assimilation of nutrients by poultry. Consequently, PL EC values exhibited a continual increase associated with higher pyrolysis temperatures. This was likely due to the loss of volatile material resulting in concentration of elements in the ash fraction. In contrast, the EC values for SW biochars were significantly lower than their raw feedstock, an average of 205 compared to 846 μS cm^{-1}. The lower EC value may be attributed to the PAM addition during the solid–liquid separation process. Although the dosage of the cationic flocculent was very low in aqueous phase, the polymer fraction can concentrate in dried sample. Its subsequent pyrolytic degradation in the solid phase may be inhibiting the dissociation of ionic compounds. The nondissociative phases may be originated by binding inorganics with oxides or other anions; formation of sulfides; or chelations with the fixed carbon forms. After pyrolysis of PAM sewage sludge, an increased association of Cu and Zn was observed with crystalline metal oxides (residual fraction), organic matter, and with sulfides (oxidizable fraction); there was a decreased association in exchangeable fractions that will contribute to the dissolved "free", hydroxide and carbonate species (He et al., 2010). The PAM additive was also observed to have an interactive affect in the thermal degradation of swine manure in their comparative thermogravimetric analyzes of flushed and solid-separated swine manure samples (Ro et al., 2009). For the current study, these hypotheses require further experimental study.

Correlation analyzes were conducted on the relationship between EC and ash contents, concentrations of K, Na, and (K + Na)

Table 1
Relative changes and statistical comparisons in physical and ultimate compositions of manure-based biochars (feedstocks: MD = dairy; FL = paved feedlot; PL = poultry litter; SW = separated swine solids; and TL = turkey litter; comparisons: temperature and feedstock columns indicate significant differences (p-value <0.05)).

	Pyrolysis temp (°C)	Feedstock					Comparisons	
		MD	FL	PL	SW	TL	Temperature	Feedstocks
pH	350[a]	*	↑	*	*	↑	700 > 350	MD, FL > PL > SW, TL
	700[b]	*	↑	↑	↑	↑		FL, PL > MD, TL > SW
EC	350	*	↓	↑	↓↓↓↓	↓↓	700 > 350	PL ≫ FL, TL > MD ≫ SW
	700	↑↑	↑↑↑	↑↑↑	*	↑↑↑		PL ≫ FL, TL > MD ≫ SW
Ash	350	↑↑↑	↑↑↑↑	↑↑↑↑	↑↑↑	↑↑↑	700 > 350	TL > SW > PL > FL > MD
	700	↑↑↑	↑↑	↑↑↑	↑↑↑	↑↑		SW, TL > PL, FL > MD
Volatile Matter	350	↓↓	↓↓	↓↓	↓↓	↓↓	350 > 700	(MD, SW) > (SW, FL) > PL, TL
	700	↓↓	↓↓↓	↓↓↓	↓↓↓↓	↓↓↓		MD > TL, FL, PL > SW
Fixed carbon	350	▲	▲	▲	▲	▲	700 > 350	PL, FL, TL, MD > SW
	700	↑↑	↑↑↑	↑	↑↑↑↑	↑		FL, PL, SW, MD > TL
HHV	350	↑	↑	↑↑	*	↑	350 > 700	(SW, MD) ⩾ (MD, FL) > PL > TL
	700	*	↓	↓	↓↓	↓		MD > FL > SW, PL, TL
C	350	↑	↑	↑	*	↑	350 > 700	(MD, FL) ⩾ (FL, SW, PL) ⩾ (SW, PL, TL)
	700	*	*	*	↓	*		MD > FL > PL, TL, SW
H	350	↓	↓↓	↓↓	↓	↓↓	350 ≫ 700	SW > MD > FL > PL, TL
	700	↓↓↓↓	↓↓↓↓	↓↓	↓↓↓↓	↓↓↓↓		PL, MD, TL, FL, SW
N	350	↑	↑↑↑	↑	↓	↑	350 > 700	(PL, TL) > (TL, FL) > (FL, SW) > MD
	700	↓↓	↓↓↓	↓↓↓	↓↓	↓↓↓		SW > (PL, TL) > (TL, FL) > (FL, MD)
S	350	↓↓↓	*	*	↓	↑	350 = 700	SW > PL, TL > FL ≫ MD
	700	↓↓	↓	*	*	↓↓		SW > PL > TL, FL ≫ MD
Biochar mass recovery ($\%_{db}$)	350	↓↓	↓↓	↓↓	↓↓	↓↓	350 > 700	SW > TL > MD, PL > FL
	700	↓↓	↓↓	↓↓	↓↓	↓↓		TL > PL, SW, MD > FL
($\%_{daf}$)	350	↓↓	↓↓↓	↓↓↓	↓↓	↓↓↓	350 > 700	(SW, MD) > TL, PL, FL
	700	↓↓↓	↓↓	↓↓	↓↓↓	↓↓		(MD, TL) > (TL, PL, SW, FL)

* = Relatively no change (<10%); ↓ or ↑ = 10–25% change; ↓↓ or ↑↑ = 25.1–50% change ↓↓↓ or ↑↑↑ = 50.1–75% change; ↓↓↓↓ or ↑↑↑↑ = 75.1–100% change; ▲ = > 100% change.
[a] Relative changes to raw feedstocks.
[b] Relative changes from 350 °C biochar.

Table 2
Manure feedstock and biochar pH, electro conductivity (EC), surface area (SA), energy content (HHV), proximate analysis, and recoveries.

Feedstock	Pyrolysis temperature (°C)	pH	EC ($\mu S\ cm^{-1}$)	SA ($m^2\ g^{-1}$)	HHV ($MJ\ kg_{db}^{-1}$)[a]	Proximate analysis			Recoveries				
						Volatile matter ($wt.\%_{db}$)	Fixed carbon ($wt.\%_{db}$)	Ash ($wt.\%_{db}$)	Mass		Carbon ($\%_{db}$)	Ash ($\%_{db}$)	Energy ($\%_{db}$)
									($\%_{db}$)	($\%_{daf}$)[b]			
Dairy (MD)	0	8.3	561	1.32	17.62 (0.26)[c]	80.7 (3.1)	4.5 (3.2)	14.8 (0.2)	–	–	–	–	–
	350	9.2	538	1.64	20.90 (0.30)	53.5 (4.3)	23.2 (3.7)	24.2 (0.5)	54.9	54.5	65.7	89.7	65.1
	700	9.9	702	186.5	18.97 (0.66)	27.7 (1.8)	34.7 (2.7)	39.5 (1.6)	35.0	26.7	42.7	93.5	37.7
Paved-feedlot (FL)	0	7.3	828	1.02	17.66 (0.32)	76.7 (0.5)	7.9 (0.6)	15.4 (0.2)	–	–	–	–	–
	350	9.1	713	1.34	20.39 (0.24)	47.9 (2.8)	23.5 (3.4)	28.7 (0.7)	51.1	45.3	60.5	95.3	59.0
	700	10.3	1140	145.2	17.23 (0.11)	19.8 (1.6)	36.3 (1.6)	44.0 (0.0)	32.2	23.2	37.5	92.0	31.4
Poultry litter (PL)	0	8.2	1255	0.57	15.11 (0.35)	74.3 (0.8)	8.8 (1.1)	16.9 (0.4)	–	–	–	–	–
	350	8.7	1405	3.93	19.03 (0.63)	42.3 (1.2)	27.0 (0.6)	30.7 (0.6)	54.3	45.9	65.9	98.7	68.4
	700	10.3	2217	50.9	14.75 (0.26)	18.3 (0.6)	35.5 (2.7)	46.2 (3.1)	36.7	23.8	40.0	100	35.8
Swine solids (SW)	0	7.8	846	0.53	19.39 (0.16)	73.6 (0.3)	5.6 (0.1)	20.9 (0.4)	–	–	–	–	–
	350	8.4	216	0.92	21.12 (0.43)	49.8 (0.6)	17.7 (1.2)	32.5 (0.9)	62.3	54.9	67.7	97.0	67.9
	700	9.5	194	4.11	15.07 (0.32)	13.4 (0.3)	33.8 (0.5)	52.9 (0.5)	36.4	23.5	33.8	92.1	28.3
Turkey litter (TL)	0	7.0	1045	1.45	15.48 (0.12)	74.0 (1.0)	5.7 (1.1)	20.3 (0.3)	–	–	–	–	–
	350	8.0	651	2.60	17.28 (0.20)	42.1 (1.5)	23.1 (1.5)	34.8 (0.1)	58.1	47.6	70.8	99.7	64.8
	700	9.9	981	66.7	14.45 (1.54)	20.8 (2.2)	29.2 (3.8)	49.9 (1.8)	39.9	25.5	44.2	98.1	37.3

[a] db = oven-dry basis.
[b] daf = oven-dry ash free basis.
[c] Standard deviation in parentheses.

for the biochars by pyrolysis temperature. Irrespective of sorting the biochars by pyrolysis temperature, there was an extremely low correlation (R^2 between <0.005 and 0.13) between % ash and EC. This implied that some elements in the ash probably occurred as insoluble oxides or hydroxides that were not capable of conducting electricity. In contrast, there was a close relationship between the EC values (Table 2) when regressed against the concentrations of K, Na (Table 5), and (K + Na). In fact, the best predictor for biochar EC values was (K + Na) combined, producing R^2 value of 0.84.

The BET surface area was found to increase with increasing temperature (Table 2). The most dramatic increases in BET surface area for a pyrolytic temperature of 700 °C were for the bovine varieties – the dairy (MD) and paved-feedlot (FL) ranging from 145 to 187 $m^2\ g^{-1}$. The PL and TL biochars were in a middle grouping, and lastly, swine manure 700 °C biochar exhibiting the lowest surface

area of 4.11 $m^2 g^{-1}$. The low surface area for the SW biochars may be attributed to the degradation behavior of the PAM. Considering potential applications, the wide range of BET among the manure biochars would potentially result in varied adsorption responses of contaminants from soils (Uchimiya et al., 2010) and may affect nutrient plant availabilities of co-applied fertilizers (Spokas et al., 2011).

When compared to the raw feedstock, increasing the pyrolytic temperature slightly increased the HHV of manure biochars when processed at 350 °C (Table 1). A further pyrolytic temperature increase caused significant decreases in the biochar energy content (Tables 1 and 2). Initially, pyrolysis increased the energy content likely due to loses of lighter, low energy density compounds along with changes in the feedstock's carbon structure. Combined, these collectively produced a more energy dense product. Further increases in temperature naturally cause additional breakdown of the carbon structure. Dairy (MD) biochars were statistically the most energy dense, which correlated to the higher carbon and lowest ash contents. Nonetheless, the manure biochars in general may be unsuited for fuel use primarily due to the high ash contents. Of note are PL and TL biochars consistently exhibiting HHV values on the lower end, correlated to their high ash contents.

3.2. Recoveries

Biochar recoveries were found to positively correlate to the feedstock ash content and negatively correlate to the feedstock VM, C, and N contents (p-value <0.05 for Pearson's correlation test). With pyrolysis primarily degrading a feedstock's VM, the more available VM, then the greater the mass losses. Accordingly, this leads to a lower biochar recovery. Likewise, high initial ash concentrations resulted in greater biochar recovery. The SW feedstock with the lowest VM and greatest ash contents generated the greatest biochar recovery of 62.3 wt.%$_{db}$ at 350 °C (Tables 1 and 2). Despite the initial feedstock having the greatest VM and lowest ash contents, the MD 350 °C biochar recovery results were within the range to the other manures (Tables 1 and 2). Different distributions were noted among the 700 °C biochars: (1) FL was the lowest, 32.2 wt.%$_{db}$; (2) MD, PL, and SW were similar with an average value of 36.0 wt.%$_{db}$; and (3) TL generated the greatest biochar recovery, 39.9 wt.%$_{db}$. Recoveries of lignocellulosic biochars like wheat, wood, and olive husk across similar temperatures were reported to range from 18%$_{daf}$ to 43%$_{daf}$ (Demirbaş, 2004; Lang et al., 2005). In our study, pyrolysis of manure feedstocks generated 5–10% more biochar product ranging 23.2–54.8%$_{daf}$ (Table 2). Our higher results were likely attributed to the increased ash content of the manure feedstocks interfering with the carbon reactions.

As with biochar mass recoveries, carbon and energy recoveries (Table 2) both decreased with pyrolysis temperature increases. Turkey litter (TL) was the best feedstock to preferentially protect carbon from thermal decomposition; it exhibited the greatest carbon recoveries at both 350 and 700 °C at 70.8 and 44.2 wt.%$_{db}$, respectively. Greater carbon recoveries were noted for the manure-based biochars when compared to pyrolyzed lignocellulosic feedstocks (Lang et al., 2005). Therefore, pyrolyzing manure feedstocks resulted in lesser amounts of volatile carbon released compared to pyrolyzing grasses and woods (Keiluweit et al., 2010). This suggested that manures had a greater propensity to retain carbon when pyrolyzed. This may be due to protective mechanisms brought on by the various inherent metals thereby changing the bond dissociation energies of inorganic and organic carbon bonds. In support, it has been shown that treating lignocellulosic biomass with inorganic salt solutions increased char production credited to alterations of reaction pathways (White et al., 2011). Similarly, lower char yields for washed rice hulls (vs. unwashed) were attributed to the loss of hydrocarbon moieties capable of promoting cross-linking reactions that foster char production (Teng and Wei, 1998). Higher levels of K and Zn were documented to contribute to increased char yield for rice husk, coir pith, and groundnut shell (Raveendran et al., 1995). The amount of energy remaining in the biochar (useful for energy balances of engineered systems) varied by feedstock type and pyrolysis temperature (Table 2). Poultry litter (PL) and SW retained the most energy in the biochar at 350 °C. As temperature increased to 700 °C, MD and TL biochars retained the greatest amount of energy. Conversely, SW biochar retained the least energy at 700 °C.

Ash recoveries for both of the tested pyrolysis temperatures ranged from 89.7% to 99.7% (Table 2). While the ash recovery would be a measure of the reproducibility and reliability of the pyrolysis procedures and system, less than 100% ash recovery was expected for the higher temperature pyrolytic runs. This was because of factors such as vaporization of P-containing compounds known to occur when temperatures approach 760 °C (Knicker, 2007). In fact, mass recovery of P in the biochar ranged from 80% to 100% among all manure biochars. Likewise, heavy metals accumulated in plants used in phytoremediation (e.g., birch and sunflower) have been reported to be lost from the solid phase during fast pyrolysis of these plants (Lievens et al., 2008). With manure feedstocks containing elevated ash contents (compared to woods and grasses), one would expect increased amounts of metal transferred from the solid phase to the gas and liquid pyrolytic products.

3.3. Elemental characteristics

Pyrolysis at 350 °C resulted in a significant increase in C (Table 3). The raw feedstocks' average C content was 44.3 ± 2.9 wt.%$_{db}$ and increased to 52.2 ± 2.5 wt.%$_{db}$. Additional increases in the pyrolytic temperature, however, slightly diminished the C content of the biochars to an average 48.8 ± 5.5 wt.%$_{db}$. Dairy (MD) and FL biochars statistically had greater C contents among the different temperature biochars (Tables 1 and 3). For reason well known (Antal and Grønli, 2003), the changes in C content occurred concurrently with the H and O losses. More than 50% of H, on a mass basis, was removed from the original feedstocks when pyrolyzing at 350 °C. Furthermore, pyrolyzing at 700 °C resulted in total H losses (mass basis) exceeding 85%. Interestingly, there was variation in the H content among the 350 °C biochars, with SW having the greatest (Tables 1 and 3). The additional increase in pyrolytic temperature caused all manure biochars to have statistically similar H contents, an average 1.10 ± 0.50 wt.%$_{db}$.

Total N content in the biochars increased initially with pyrolysis at 350 °C; there was one exception with SW (Tables 1 and 3). Initial N content ranged from 2.29 ± 0.03 wt.%$_{db}$ (MD) to 4.11 ± 0.78 wt.%$_{db}$ (SW). The N content increased for the 350 °C MD, PL, and TL biochars with an average of 17.8% (Tables 1 and 3). The greatest increase was observed for the FL 350 °C biochar. This may be related to recalcitrant N occurring in heterocyclic compounds (Kazi et al., 2011). On the other hand, the SW biochars exhibited a decrease in N concentration. However, the mechanism for this observation is not well understood. All N concentrations decreased for the 700 °C pyrolytic temperature to values less than the initial feedstock (Table 3). There were statistical variations among N contents across the biochars: MD biochars consistently had the lowest N content, whereas, SW 350 °C was similar to FL on the lower concentrations, but statistically had the greatest N concentration among the 700 °C biochars. On a mass basis, N mass losses for the 350 °C biochars ranged between 21.4% (for FL) and 46.4% (for SW). As temperature increased to 700 °C, these losses increased to an average 77.5% relative to the feedstocks. Nitrogen losses may have been due to emission of ammonia and other volatile organic compounds containing N during pyrolysis as well as N_2 (Novak et al., 2009; Ro et al., 2010; Sheth and Bagchi, 2005).

Table 3
Elemental composition and atomic ratios of various manure feedstocks (pyrolysis temperature = 0) and biochars.

Feedstock	Pyrolysis temperature (°C)	Elemental composition (wt.%$_{db}$)[b]					Atomic ratios		
		C	H	N	S	O[a]	H/C	O/C	(O + N)/C
Dairy (MD)	0	46.52 (0.06)[c]	5.49 (0.01)	2.29 (0.03)	0.25 (0.02)	33.20 (0.69)	1.42	0.54	0.58
	350	55.80 (1.65)	4.29 (0.08)	2.60 (0.14)	0.11 (0.02)	18.73 (1.39)	0.92	0.25	0.29
	700	56.67 (0.69)	0.94 (0.06)	1.51 (0.03)	0.15 (0.02)	4.13 (0.23)	0.20	0.05	0.08
Paved-feedlot (FL)	0	45.05 (0.08)	5.47 (0.02)	2.37 (0.03)	0.44 (0.00)	32.47 (0.32)	1.46	0.54	0.59
	350	53.32 (0.60)	4.05 (0.09)	3.64 (0.05)	0.45 (0.02)	15.70 (0.66)	0.91	0.22	0.28
	700	52.41 (0.61)	0.91 (0.07)	1.70 (0.04)	0.40 (0.06)	7.20 (0.53)	0.21	0.10	0.13
Poultry litter (PL)	0	42.15 (0.02)	5.23 (0.03)	3.67 (0.06)	0.58 (0.02)	34.80 (0.70)	1.49	0.62	0.69
	350	51.07 (0.49)	3.79 (0.16)	4.45 (0.22)	0.61 (0.03)	15.63 (0.23)	0.89	0.23	0.30
	700	45.91 (1.44)	1.98 (2.13)	2.07 (0.18)	0.63 (0.14)	10.53 (0.60)	0.52	0.17	0.21
Swine solids (SW)	0	47.42 (0.08)	6.01 (0.22)	4.11 (0.78)	0.94 (0.03)	26.07 (0.15)	1.52	0.41	0.49
	350	51.51 (0.88)	4.91 (0.10)	3.54 (0.02)	0.80 (0.01)	11.10 (0.35)	1.14	0.16	0.22
	700	44.06 (0.13)	0.74 (0.11)	2.61 (0.07)	0.85 (0.03)	4.03 (0.21)	0.20	0.07	0.12
Turkey litter (TL)	0	40.45 (0.20)	5.04 (0.03)	3.43 (0.39)	0.48 (0.08)	30.23 (0.21)	1.50	0.56	0.63
	350	49.28 (2.82)	3.60 (0.11)	4.07 (0.58)	0.55 (0.06)	15.40 (0.71)	0.88	0.23	0.31
	700	44.77 (3.19)	0.91 (0.03)	1.94 (0.24)	0.41 (0.11)	5.80 (1.71)	0.24	0.10	0.13

[a] O directly measured.
[b] db = oven-dry basis.
[c] Standard deviation in parentheses.

Consequently, for all 350 and 700 °C biochars, NH_4–N concentrations were either below detection limits or less than 0.01 wt.%$_{db}$ (for SW and TL). The NO_3–N content among all biochars ranged from 0.1 to 3.5 mg kg$_{db}^{-1}$. For all manures except MD, this was more than a 90% decrease from initial NO_3–N values (74.1 mg kg$_{db}^{-1}$ for PL; 16.3 mg kg$_{db}^{-1}$ for TL; 3.6 mg kg$_{db}^{-1}$ for SW; and 1.8 mg kg$_{db}^{-1}$ for FL). For MD biochars, the NO_3–N content increased by 30% from its feedstock value of 1.4 mg kg$_{db}^{-1}$.

For the combustible S component, a pyrolytic increase in temperature was found not to significantly alter the S concentrations between the 350 and 700 °C biochars (Table 1). This may largely be influenced to little to no change in the FL and PL biochar S content (Table 1). While there were detectable differences among S contents of the biochar varieties, MD biochars had drastically less S. The SW biochars's S contents were constantly the greatest of the study. For the MD and SW biochars, pyrolysis at 350 °C caused an initial decrease in S content that stabilized with additional temperature increases (Tables 1 and 3). Biochar from TL had an S content that experienced a similar phenomenon much like the N content (Tables 1 and 3). These mixed results were also reported by Gaskin et al. (2008); however, no reasoning was provided for their occurrence. Knudsen et al. (2004) reported the thermal decomposition of organic S during pyrolysis up to 400 °C; at higher temperatures approaching 700 °C, the S as insoluble sulfides in the biochar matrix were altered by the addition of native S to unsaturated sites on the biochar surface. For the manure-based biochars, these phenomena may be related to S-containing volatile organic compounds lost at 350 °C in combination or separate from the S in certain organic compounds being more resistant to S-bond breakages. As such, this renders the S as less plant-available. Despite the varied S content response, S was sensitive to major vapor-phase mass losses. Compared to N, there was a greater loss of S, especially for MD biochars. However, a similar response was observed: Additional temperature increases resulted in greater losses of these elements. Among the feedstocks, MD biochars experienced the greatest mass loss of S for both temperatures with more than 75% released. Biochar made from turkey litter at 350 °C exhibited the lowest S mass loss of 32.8%. Organic sulfur losses to the vapor phase during pyrolysis have been primarily identified as carbonyl sulfide (Ro et al., 2010).

Atomic ratios, because of dissimilar O and H losses, varied as a function of feedstock and pyrolysis temperature (Table 3; Fig. 1)

Table 4
Mean mineral analyses of manure feedstocks (pyrolysis temperature = 0) and biochars.

Feedstock	Pyrolysis temperature (°C)	P (g kg$_{db}^{-1}$)[a]	Soluble P (g kg$_{db}^{-1}$)	Al (g kg$_{db}^{-1}$)	Ca (g kg$_{db}^{-1}$)	Fe (g kg$_{db}^{-1}$)	K (g kg$_{db}^{-1}$)	Mg (g kg$_{db}^{-1}$)	Na (g kg$_{db}^{-1}$)	Cr (mg kg$_{db}^{-1}$)	Mn (mg kg$_{db}^{-1}$)
Dairy (MD)	0	5.61 (0.31)[b]	1.47 (0.15)	1.61 (0.21)	16.0 (0.3)	2.29 (0.17)	6.70 (1.4)	6.94 (0.36)	2.51 (1.32)	2.97 (0.15)	305 (15)
	350	10.0 (0.3)	0.38 (0.05)	2.30 (0.04)	26.7 (1.3)	3.64 (0.16)	14.3 (2.2)	12.2 (0.73)	5.62 (0.85)	6.58 (0.69)	525 (22)
	700	16.9 (0.5)	0.10 (0.0)	4.92 (0.22)	44.8 (1.1)	6.48 (0.19)	23.1 (0.8)	20.6 (0.4)	8.79 (0.44)	10.1 (0.6)	867 (22)
Paved-feedlot (FL)	0	7.07 (1.9)	3.07 (0.15)	1.31 (0.33)	14.0 (0.3)	1.55 (0.32)	20.2 (0.2)	4.55 (0.3)	2.80 (0.11)	2.37 (0.40)	179 (11)
	350	11.4 (0.2)	0.46 (0.02)	1.86 (0.08)	22.7 (0.4)	2.26 (0.20)	32.0 (0.1)	7.66 (0.14)	4.88 (0.15)	4.40 (1.5)	259 (7.1)
	700	17.6 (0.3)	0.18 (0.2)	3.95 (0.09)	35.0 (0.9)	3.45 (0.19)	49.1 (0.6)	12.2 (0.2)	7.60 (0.14)	6.82 (1.1)	388 (8.6)
Poultry litter (PL)	0	13.9 (0.6)	2.90 (0.20)	0.400 (0.02)	18.0 (0.7)	0.68 (0.03)	30.5 (2.2)	6.40 (0.61)	9.20 (0.41)	3.07 (0.25)	435 (37)
	350	20.8 (0.5)	0.43 (0.06)	0.399 (0.01)	26.6 (0.1)	1.32 (0.36)	48.5 (4.0)	9.46 (0.47)	14.8 (0.92)	5.00 (0.44)	640 (23)
	700	31.2 (0.0)	0.90 (0.14)	0.988 (0.02)	40.2 (0.2)	1.89 (0.13)	74.0 (3.2)	14.5 (0.0)	22.2 (0.51)	6.86 (0.03)	948 (22)
Swine solids (SW)	0	24.7 (0.8)	11.0 (1.3)	0.786 (0.04)	23.9 (1.1)	3.15 (0.42)	10.9 (0.3)	15.0 (0.5)	3.62 (0.15)	14.9 (0.4)	907 (31)
	350	38.9 (0.4)	0.39 (0.08)	1.17 (0.02)	39.1 (0.5)	4.84 (0.04)	17.8 (0.2)	24.4 (0.4)	5.98 (0.15)	24.8 (0.2)	1453 (6.8)
	700	59.0 (2.7)	0.06 (0.01)	2.14 (0.02)	61.5 (3.2)	7.48 (0.45)	25.7 (2.5)	36.9 (2.7)	9.35 (0.90)	36.5 (2.2)	2240 (97)
Turkey litter (TL)	0	16.1 (1.1)	9.11 (0.48)	1.17 (0.05)	24.1 (3.3)	1.47 (0.24)	25.0 (0.2)	5.27 (0.33)	3.80 (0.16)	4.80 (0.31)	425 (23)
	350	26.2 (1.1)	1.06 (0.07)	2.14 (0.52)	40.4 (1.1)	2.78 (0.22)	40.1 (4.4)	8.50 (0.39)	6.60 (0.11)	8.31 (2.0)	710 (33)
	700	36.6 (3.8)	1.75 (1.16)	3.84 (0.33)	56.1 (6.8)	3.65 (0.50)	55.9 (6.8)	12.4 (1.2)	9.24 (0.65)	10.4 (0.7)	986 (100)

[a] db = oven-dry basis.
[b] Standard deviation in parentheses.

where all molar ratios demonstrated a decreasing trend with increasing pyrolysis temperature. These trends were attributed to (1) removal of polar surface functional groups and (2) instances of higher degree of carbonization resulting in formation of more aromatic structures, which are more recalcitrant OC structures (Chen et al., 2008; Keiluweit et al., 2010; Lehmann and Joseph, 2009; Uchimiya et al., 2010). Following that logic, the higher temperature biochars compared to their lower temperature counterparts would be less polar and have greater aromaticity leading to a more hydrophobic character. Of note are the trends for MD, FL, and TL: these ratios continually overlapped suggesting similar behaviors (Fig. 1). Among the 700 °C biochars, PL with the greatest H/C ratio would be expected to have the least aromaticity. Among the 350 °C biochars, SW with a lower O/C ratio would be expected to be the least polar.

3.4. Nutrient characteristics

Pyrolysis concentrated mineral and heavy metals (with some notable exceptions for Cd and Pb) (Tables 4 and 5). Within a pyrolysis temperature, the order of concentration of an individual component (e.g., greatest to lowest) remained constant when compared to the order of the concentrations in the raw feedstocks. Using P as an example, the concentrations from greatest to least for the raw feedstocks were SW > TL > PL > FL > MD; a similar ranking occurred within the 350 and 700 °C biochars. Consequently, there was no correlation between initial feedstock nutrient concentrations and the % increase in concentration. Thus, under the pyrolysis conditions employed in this study, the lack of correlation implied that initial feedstock nutrient composition did not affect pyrolysis reactions equally and had no significant effect on final biochar compositions; as such, initial concentrations could not be used to quantitatively predict final biochar nutrient contents.

By being rich in minerals important for plant growth like P, manure-based biochars may be better suited as an alternative fertilizer. The P-content of all manure 350 °C biochars increased from the feedstock concentrations by 50–80%; for the 700 °C biochars compared to feedstocks, P content increased 125–202%. In spite of these increases, further studies are required to determine their plant P availability status. This is especially true when water

Table 5
Mean heavy metal analyzes of manure feedstocks (pyrolysis temperature = 0) and biochars.

Feedstock	Pyrolysis temperature (°C)	As (mg kg_{db}^{-1})[a]	Cd (mg kg_{db}^{-1})	Cu (mg kg_{db}^{-1})	Mo (mg kg_{db}^{-1})	Ni (mg kg_{db}^{-1})	Pb (mg kg_{db}^{-1})	Zn (mg kg_{db}^{-1})
Dairy (MD)	0	0.23 (0.12) [b]	0.03 (0.06)	54.5 (2.6)	3.70 (0.10)	5.77 (0.06)	1.20 (0.17)	220 (5.9)
	350	0.78 (0.35)	0.18 (0.01)	99.0 (6.2)	7.83 (0.29)	16.1 (2.8)	0.89 (0.32)	361 (18)
	700	1.05 (0.30)	BD[c]	163 (3.0)	10.0 (0.7)	25.3 (3.5)	0.46 (0.57)	423 (43)
Paved-feedlot (FL)	0	1.13 (0.21)	0.07 (0.06)	36.7 (2.1)	2.73 (0.42)	2.87 (0.21)	1.70 (0.35)	223 (11)
	350	1.18 (0.17)	0.20 (0.02)	91.7 (19)	6.22 (0.60)	4.21 (1.40)	0.71 (0.72)	359 (10)
	700	2.32 (1.21)	0.02 (0.01)	136 (6.4)	6.33 (0.17)	6.56 (0.93)	0.19 (0.16)	448 (10)
Poultry litter (PL)	0	19.6 (2.6)	0.13 (0.06)	146 (69)	5.20 (0.62)	4.10 (0.62)	0.53 (0.25)	483 (30)
	350	25.1 (1.7)	0.25 (0.01)	213 (4.4)	11.0 (0.1)	7.79 (0.44)	1.03 (0.49)	712 (23)
	700	29.5 (0.1)	0.11 (0.0)	310 (15)	13.0 (0.2)	11.4 (0.31)	1.09 (0.53)	1010 (16)
Swine solids (SW)	0	0.72 (0.14)	0.27 (0.06)	918 (18)	10.9 (0.5)	9.88 (0.37)	1.20 (0.09)	1961 (65)
	350	0.90 (0.10)	0.57 (0.06)	1538 (21)	18.3 (0.3)	16.2 (0.2)	2.60 (0.10)	3181 (46)
	700	1.64 (0.35)	0.23 (0.09)	2446 (104)	27.4 (0.7)	25.6 (1.6)	BD	4981 (130)
Turkey litter (TL)	0	102 (3.0)	0.54 (0.12)	349 (20)	4.79 (1.67)	17.1 (0.3)	0.85 (0.74)	424 (25)
	350	138 (30)	0.72 (0.03)	535 (42)	7.16 (1.16)	28.6 (1.7)	2.01 (0.47)	690 (22)
	700	166 (22)	0.73 (0.19)	762 (81)	10.1 (0.8)	39.6 (3.7)	BD	909 (99)

[a] db = oven-dry basis.
[b] Standard deviation in parentheses.
[c] BD = below detection limit.

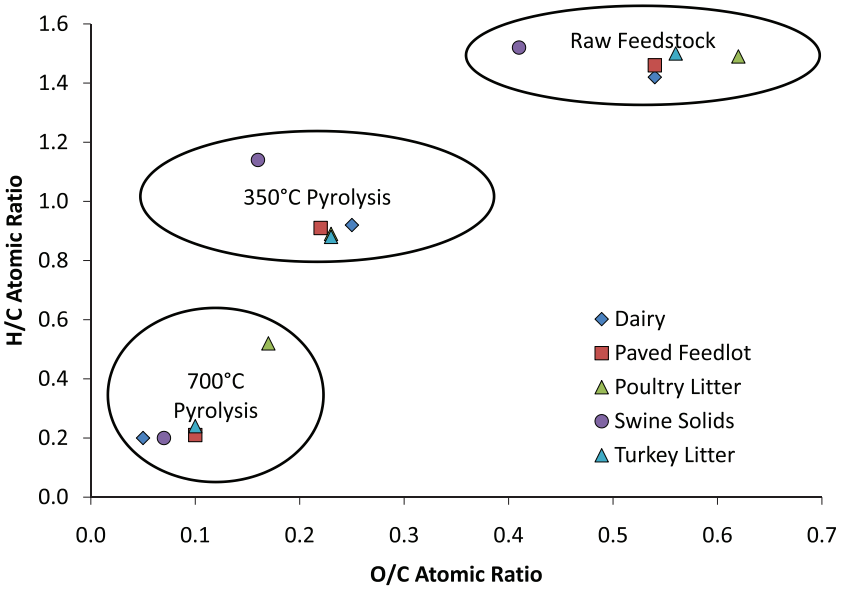

Fig. 1. van Krevelen diagram for manure-based feedstocks and 350 and 700 °C biochars.

soluble P continually decreased to values 0.5–31% of raw feedstock soluble P values (Table 4). The SW feedstock had the second greatest contribution of water soluble P to total P at 44.5% (TL feedstock was at 56.6%); this was largely attributed to the solid–liquid separation system separating both flushed material and a phosphate precipitated sludge. The SW biochars had less than 1% contribution of soluble P to total P, which was the lowest among all the biochars. This is interesting and suggests some investigations are required to fully understand the impact of pyrolyzed PAM on pyrolysis mechanisms and biochar characteristics.

The concentrations for elements regulated under 40 C.F.R. §503 (e.g., As, Cd, Cu, Mo, Ni, Zn) were lower than listed ceiling concentrations (Table 5) (EPA, 2005). The one exception was for TL biochars; the As concentration in the raw feedstock was already above acceptable concentrations; thus, pyrolyzing turkey litter (TL) could worsen the situation. Regardless, annual loading rates should be monitored if there are intentions of long term repeated soil applications of manure biochars.

In some heavy metal cases, the biochar concentrations decreased with increases in temperature (e.g., Cd for all but TL biochars and Pb for SW and TL biochars). This was not an unusual occurrence because pyrolysis of heavy metal contaminated plants used in phytoremediation revealed that Cd can be lost in gas and oil phases– 18% at 400 °C up to 89% at 600 °C (Lievens et al., 2008). In contrast, Pb, Zn, and Cu did not exhibit losses to these same phases. However, Pb vaporization has been reported during incineration of municipal waste at temperatures as low as 650 °C (Asthana et al., 2010). As such, the heavy metal concentration would need to be monitored for the other product phases of pyrolysis. Fortunately, with respect to heavy metal concentrations in the biochar phase, the low concentrations implied that the biochars generated at both temperatures (except As for the TL biochars) would have minimal impact on increasing soil heavy metal concentrations in a singular short term application. However, suitability of other biochars as a soil amendment would depend on feedstock selection and initial nutrient concentrations.

3.5. FTIR characteristics

The FTIR spectra are presented in supplementary material (Supplementary Fig. 1a–c) for raw manure feedstocks and biochars produced at 350 and 700 °C; descriptions for peak assignments are provided in Table 6. For the feedstocks, the broad band near 3300 cm^{-1} was attributed to the stretching vibration of hydrogen-bonded hydroxyl groups (Keiluweit et al., 2010). The asymmetric (2935 cm^{-1}) and symmetric (2885 cm^{-1}) C–H stretching bands were associated with aliphatic functional groups. Relative to the other manures investigated, sharper C–H stretching bands for the SW feedstock suggested a more aliphatic nature. The C=O stretching for carboxyl, aldehyde, ketone and ester were identified

Table 6
Pyrolysis temperature effects on relative change in FTIR wave number identification of manure feedstocks (pyrolysis temp = 0) and biochars (feedstocks: MD = dairy; FL = paved feedlot; PL = poultry litter; SW separated swine solids; and TL = turkey litter).

Wave number (cm^{-1})	Pyrolysis temp (°C)	Feedstock					Characteristic vibrations (functionality)
		MD	FL	PL	SW	TL	
3500–3200	0	*	*	*	*	*	O–H stretching (water, hydrogen-bonded hydroxyl Keiluweit et al. (2010))
	350	↓	↓	↓	↓	↓	
	700	–	–	–	–	–	
2935; 2885	0	*	*	*	*	*	C–H stretching (aliphatic CH_x; 2935-asymmetric, 2885- symmetric Keiluweit et al. (2010))
	350	↓	↓	↓	↓	↓	
	700	–	–	–	–	–	
1740-1700	0	*	*	*	*	*	C=O stretching (carboxyl, aldehyde, ketone, ester Keiluweit et al. (2010))
	350	↑	↑	↑	↑	↑	
	700	–	–	–	–	–	
1653-1645	0	*	*	*	*	*	N–C=O (amide I: carbonyl stretching vibration in peptide bond (Jiang et al. (2004))
	350	↓	↓	*	–	↓	
	700	–	–	↓↓	–	↓↓	
1600-1595	0	–	–	–	*	–	CC=C, C=O, C=N (aromatic components conjugated ketones and quinones Keiluweit et al. (2010);
	350	*	*	*	↓	*	amide, amine Xiu et al. (2010))
	700	–	–	↓↓	–	↓↓	
1514	0	*	*	*	*	*	C=C, N–H (secondary aromatic amines, pyridine rings Das et al. (2009))
	350	–	–	↓	↓↓	↓	
	700	–	–	–	–	–	
1440	0	*	*	*	*	*	C=C stretching; –C–H_2 bending (lignin carbohydrate Keiluweit et al. (2010))
	350	↑	↑	*	↑	↑	
	700	–	–	↑	–	↓	
1375	0	–	–	*	*	*	O–H bending (phenolic; ligneous syringyl Keiluweit et al. (2010))
	350	–	–	↑	*	↑	
	700	–	–	↑	–	↑	
1110	0	–	–	–	–	–	Symmetric C–O stretching (C–O-C in lignocelluloses Keiluweit et al. (2010))
	350	–	–	–	*	–	
	700	–	–	–	↓↓	–	
1100–950	0	*	*	*	*	*	P–O (asymmetric and symmetric stretching of PO_2 and $P(OH)_2$ in phosphate Jiang et al. (2004))
	350	*	*	*	*	*	
	700	*	*	*	*	*	
1030	0	*	*	*	*	*	Symmetric C–O stretching (cellulose; hemicellulose; methoxy groups of lignin Keiluweit et al. (2010))
	350	↓	↓	↓	*	↓	
	700	↓↓	↓↓	↓*	*	↑	
885	0	–	*	*	–	*	C–H bending (aromatic CH out-of-plane deformation Keiluweit et al. (2010))
	350	*	↑	↑	*	*	
	700	↑	↓	↓	↓	↑	
781	0	–	–	*	–	*	Pyridine (pyridine ring vibration and C–H deformation Das et al. (2009))
	350	–	–	↑	–	↑	
	700	–	–	–	–	–	

* = identified peak or area; ↓ = decrease in intensity from previous row (within a manure feedstock); ↓↓ = major decrease in intensity from previous row (within manure feedstock) but still identifiable; ↑ = increase in intensity from previous row (within manure feedstock); – = unidentifiable.

in the band width 1740–1700 cm^{-1}. In addition to these band assignments, C=O stretching vibrations for amides were noted at 1645–1653 cm^{-1} (Calderón et al., 2006; Das et al., 2009). Absorption band of amide in this region likely results from carbonyl stretching vibration in the peptide bond, rather than the N–H bending and C–N stretching that appear at lower wave number (Jiang et al., 2004). In FTIR analysis of manures, amides are often assigned as the protein-specific band, as opposed to the primary amines (Calderón et al., 2006). Considering the high P content of manure chars (Table 5), the broad band near 1070 cm^{-1} likely resulted from P-containing functional groups, most importantly the P–O bond of phosphate (Wen et al., 2007). Both organic (phosphate mono- and di-esters) and inorganic (orthophosphate and its oligomers) phosphate (Jiang et al., 2004) can contribute to the intense band in this region. Additional inorganic components such as sulfates and silicates can also contribute to the broad and intensive peak at 970–1200 cm^{-1} (Wen et al., 2007). The pinnacle of this region at band 1030 cm^{-1} was attributed to the symmetric C–O stretching for cellulose, hemicellulose, and lignin, which could be found in bedding material and partially digested feed (Calderón et al., 2006; Keiluweit et al., 2010). Two identifiable peaks were unique to the MD and FL feedstocks; at 1240 cm^{-1}, there were C–H stretching and OH deformation of COOH along with C–O stretching of aryl esters; at 1160 cm^{-1}, there was asymmetric C–O stretching characteristic of C–O–C in cellulose and hemicelluloses. These peaks may be attributable to the pyrolysis of the undigested or partially digested corn stalk bedding (FL) and hay silage for feeding (MD). For PL and SW, and TL to some degree (Suppl. Fig. 1a–c), a peak centered at 1514 cm^{-1} likely arose from secondary aromatic amines, such as C=C stretching of pyridine rings (Das et al., 2009). The O–H bending of phenols were identified at band 1375 cm^{-1} for TL, PL, and SW feedstocks.

As noted for the FTIR spectra for the 350 °C biochars, implementing pyrolysis at lower temperatures resulted in dehydration, beginnings of bond breakages, and transformational products (Table 6). All 350 °C biochar FTIR spectra indicated decreases in the hydrogen-bonded hydroxyl groups (i.e., dehydration). In addition, these spectra had less prominent bands associated with the aliphatic functional groups. Some deformation in the aliphatic bands was observed for the 350 °C SW biochar; however, the spectra for the 350 °C SW biochar had the sharpest aliphatic bands (among the manure chars). This suggested that greater pyrolysis temperatures would be required, relative to other manures, to begin significant degradation of swine-based aliphatic C–H. Concurrently, stretching vibrations for amides and secondary aromatic amines/pyridine rings were either unidentifiable or decreased. There was a presence of amides associated with TL and PL biochars, which was supported by the greater N concentrations (Table 3). The symmetric (1030 cm^{-1}) and asymmetric (1160 cm^{-1}) stretching of C–O bonds began to disappear for all biochars as well suggesting degradation of cellulose, hemicelluloses, and lignin. Particularly for FL and MD, peaks also decreased attributable to C–H stretching and OH deformation of COOH and C–O stretching of aryl esters (1240 cm^{-1}).

The pyrolysis of manure at 350 °C generated transformational products. In particular, all biochars began to increase aromatic C=C stretching (1440 cm^{-1}) and out-of-plane deformation by aromatic C–H groups (885 cm^{-1}). Both PL and TL exhibited FTIR spectral behavior suggesting increasing (1) symmetric C–O stretching (1110 cm^{-1}), (2) aromatic C=C stretching and C=O stretching of conjugated ketones and quinones (1600 cm^{-1}), and (3) O–H bending of phenols (1375 cm^{-1}). These changes were attributable to the transformation products of lignin and cellulose. A minor peak at 781 cm^{-1} was assigned to the ring vibration of pyridines (Das et al., 2009). Pyridine is one of the heterocyclic nitrogen compounds commonly observed during fast pyrolysis of manures (Kazi et al., 2011). For FL, MD, and SW (Suppl. Fig. 1b and c), the peak increase was attributable to C=C and C=N functional groups (centered at 1595 cm^{-1}) (Xiu et al., 2010).

By 700 °C, most of the spectral features, except for the region attributable to phosphate groups, were lost and the spectrum began to resemble pure graphite. This was in agreement with progressive upward shift resulting from low-energy electron excitations of condensed aromatic structures (Keiluweit et al., 2010). As such, aliphatics and secondary aromatic amines were fully degraded in the 700 °C biochars along with C=O associated with carboxyl, ketones, and esters. Yet, the 700 °C TL and PL biochars still had identifiable C=O stretching of ketones and O–H bending of phenols. The peak near 1420 cm^{-1} could also arise from calcite and other carbonate mineral components (CO_3^{2-}) of manure biochar (Cao and Harris, 2010).

Overall, FTIR spectra for manure biochars followed the trend previously observed for wood and grass chars (Keiluweit et al., 2010) with additional contributions from P- and N-containing groups: (1) disappearance of lignin, cellulose, hemicellulose, and protein components of the source material; (2) formation and subsequent disappearance of transformation products; and (3) growth of aromatic structure. Of five manure samples investigated, spectral features were similar for (1) TL and PL and (2) FL and MD, but were distinct for SW. A sharp increase in the aromatic peaks for biochars produced at 300–500 °C was also observed in previous solid state ^{13}C NMR analyzes of swine manure chars (Cantrell and Martin, 2011; Cao et al., 2011).

4. Conclusions

Pyrolysis of manures across animal varieties generates an alkaline biochar with predominately stable, aromatic carbon structures rich in inorganic minerals. Elemental and FTIR analyzes demonstrated physicochemical variations and similarities. Spectra qualified the formation and disappearance of transformation products with increased pyrolysis temperature and were similar for (1) TL and PL and (2) FL and MD, but distinct for SW biochars. High biochar mass recovery strongly correlated to the feedstock proximate and C/N elemental characteristics. Concentration of non-volatile minerals like P and K may prove beneficial for use of manure-based biochar as an alternative fertilizer.

Acknowledgements

The authors greatly acknowledge the following for their help in providing livestock manure samples: Dr. Ray Campbell and Terra Blue, Inc.; Dr. Bryan Woodbury with USDA-ARS Clay Center, NE; Courtney Miller and Glenview Farm in MD; Jimmy Meyers chicken farm in SC; and David Kirk turkey farm in SC. The authors are grateful to Jerry Martin II, Jarrod Miller, William Brigman, Mel Johnson, Elizabeth Ford, and Don Watts for aid in sample collection and analyzes. Mention of a trade name, proprietary product, or vendor is for information only and does not guarantee or warrant the product by the USDA and does not imply its approval to the exclusion of other products or vendors that may also be suitable.

Appendix A. Supplementary data

Supplementary data associated with this article can be found, in the online version, at doi:10.1016/j.biortech.2011.11.084.

References

Antal Jr., M.J., Grønli, M., 2003. The art, science, and technology of charcoal production. Ind. Eng. Chem. Res. 42, 1619–1640.

Asthana, A., Falcoz, Q., Sessiecq, P., Patisson, F., 2010. Modeling kinetics of Cd, Pb, and Zn vaporization during municipal solid waste bed incineration. Ind. Eng. Chem. Res. 49, 7605–7609.

ASTM, 2006. Petroleum Products, Lubricants, and Fossil Fuels: Gaseous Fuels, Coal, and Coke. ASTM International, W. Conshohocken, PA.

Bourke, J., Manley-Harris, M., Fushimi, C., Dowaki, K., Nunoura, T., Antal Jr., M.J., 2007. Do all carbonized charcoals have the same chemical structure?. 2. A model of the chemical structure of carbonized charcoal. Ind. Eng. Chem. Res. 46, 5954–5967.

Calderón, F.J., McCarty, G.W., Reeves III, J.B., 2006. Pyrolysis-MS and FT-IR analysis of fresh and decomposed dairy manure J. Anal. Appl. Pyrolysis 76 14-23.

Cantrell, K.B., Ducey, T., Ro, K.S., Hunt, P.G., 2008. Livestock waste-to-bioenergy generation opportunities. Bioresour. Technol. 99, 7941–7953.

Cantrell, K.B., Martin, J.H., 2011. State-space temperature regulation development of biochar production Part II: Application to manure processing via pyrolysis. J. Sci. Food Agric. DOI 10.1002/jsfa.4617.

Cao, X., Harris, W., 2010. Properties of dairy-manure-derived biochar pertinent to its potential use in remediation. Bioresour. Technol. 101, 5222–5228.

Cao, X., Ro, K.S., Chappell, M., Li, Y., Mao, J., 2011. Chemical structures of swine-manure chars produced under different carbonization conditions investigated by advanced solid-state ^{13}C nuclear magnetic resonance (NMR) spectroscopy. Energy Fuel 25, 388–397.

Chen, B., Zhou, D., Zhu, L., 2008. Transitional adsorption and partition of nonpolar and polar aromatic contaminants by biochars of pine needles with different pyrolytic temperatures. Environ. Sci. Technol. 42, 5137–5143.

Das, D.D., Schnitzer, M.I., Monreal, C.M., Mayer, P., 2009. Chemical composition of acid–base fractions separated from bio-oil derived by fast pyrolysis of chicken manure. Bioresour. Technol. 100, 6524–6532.

Demirbaş, A., 2004. Effects of temperature and particle size on bio-char yield from pyrolysis of agricultural residues. J. Anal. Appl. Pyrolysis 72, 243–248.

EPA, 2005. Title 40- Protection of Environment. Standards for the use or disposal of sewage sludge. Code of Federal Regulations. Title 40, Pt. 503. US Environmental Protection Agency, Washington, D.C.

Gaskin, J.W., Steiner, C., Harris, K., Das, K.C., Bibens, B., 2008. Effect of low-temperature pyrolysis conditions on biochar for agricultural use. Trans. ASABE 51, 2061–2069.

He, Y.D., Zhai, Y.B., Li, C.T., Yang, F., Chen, L., Fan, X.P., Peng, W.F., Fu, Z.M., 2010. The fate of Cu, Zn, Pb and Cd during the pyrolysis of sewage sludge at different temperatures. Environ. Technol. 31, 567–574.

Jiang, W., Saxena, A., Song, B., Ward, B.B., Beveridge, T.J., Myneni, S.C.B., 2004. Elucidation of functional groups on gram-positive and gram-negative bacterial surfaces using infrared spectroscopy. Langmuir 20, 11433–11442.

Kazi, Z.H., Schnitzer, M.I., Monreal, C., Mayer, P., 2011. Separation and identification of heterocyclic nitrogen compounds in bio-oil derived by fast pyrolysis of chicken manure. J. Environ. Sci. Health: B 46, 51–61.

Keiluweit, M., Nico, P.S., Johnson, M.G., Kleber, M., 2010. Dynamic molecular structure of plant biomass-derived black carbon (biochar). Environ. Sci. Technol. 44, 1247–1253.

Knicker, H., 2007. How does fire affect the nature and stability of soil organic nitrogen and carbon?. A review. Biogeochemical 85, 91–118.

Knudsen, J.N., Jensen, P.A., Lin, W., Frandsen, F.J., Dam-Johnson, K., 2004. Sulfur transformations during thermal conversion of herbacous biomass. Energy Fuel 18, 810–819.

Lang, T., Jensen, A.D., Jensen, P.A., 2005. Retention of organic elements during solid fuel pyrolysis with emphasis on the peculiar behavior of nitrogen. Energy Fuel 19, 1631–1643.

Lehmann, J., Joseph, S., 2009. Biochar for Environmental Management: Science and Technology. Earthscan, Sterling, VA.

Lievens, C., Yperman, J., Vangronsveld, J., Carleer, R., 2008. Study of the potential valorisation of heavy metal contaminated biomass via phytoremediation by fast pyrolysis: Part I. Influence of temperature, biomass species and solid heat carrier on the behaviour of heavy metals. Fuel 87, 1894–1905.

Novak, J.M., Lima, I., Baoshan, X., Gaskin, J.W., Steiner, C., Das, K.C., Watts, D.W., Busscher, W.J., Schomberg, H., 2009. Characterization of designer biochar produced at different temperatures and their effects on a loamy sand. Ann. Environ. Sci. 3, 195–206.

Raveendran, K., Ganesh, A., Khilar, K.C., 1995. Influence of mineral matter on biomass pyrolysis characteristics. Fuel 74, 1812–1822.

Ro, K.S., Cantrell, K.B., Hunt, P.G., 2010. High-temperature pyrolysis of blended animal manures for producing renewable energy and value-added biochar. Ind. Eng. Chem. Res. 49, 10125–10131.

Ro, K.S., Cantrell, K.B., Hunt, P.G., Ducey, T.F., Vanotti, M.B., Szogi, A.A., 2009. Thermochemical conversion of livestock wastes: carbonization of swine solids. Bioresour. Technol. 100, 5466–5471.

Sheth, A.C., Bagchi, B., 2005. Investigation of nitrogen-bearing species in catalytic steam gasification of poultry litter. J. Air Waste Manage. Assoc. 55, 619–628.

Singh, B., Singh, B.P., Cowie, A.L., 2010. Characterisation and evaluation of biochars for their application as a soil amendment. Aust. J. Soil Res. 48, 516–525.

Spokas, K.A., Cantrell, K.B., Novak, J.M., Archer, D.W., Ippolito, J.A., Collins, H.P., Boateng, A.A., Lima, I.M., Lamb, M.C., McAloon, A.J., Lentz, R.D., Nichols, K.A., 2011. Biochar: A synthesis of its agronomic impact beyond carbon sequestration. J. Environ. Qual. doi: 10.2134/jeq2011.0069.

Teng, H., Wei, Y., 1998. Thermogravimetric studies on the kinetics of rice hull pyrolysis and the influence of water treatment. Ind. Eng. Chem. Res. 37, 3806–3811.

Uchimiya, M., Lima, I.M., Thomas Klasson, K., Chang, S., Wartelle, L.H., Rodgers, J.E., 2010. Immobilization of heavy metal ions (CuII, CdII, NiII, and PbII) by broiler litter-derived biochars in water and soil. J. Agric. Food Chem. 58, 5538–5544.

Wen, B., Zhang, J., Zhang, S., Shan, X., Khan, S.U., Xing, B., 2007. Phenanthrene sorption to soil humic acid and different humin fractions. Environ. Sci. Technol. 41, 3165–3171.

White, J.E., Catallo, W.J., Legendre, B.L., 2011. Biomass pyrolysis kinetics: a comparative critical review with relevant agricultural residue case studies. J. Anal. Appl. Pyrolysis 91, 1–33.

Xiu, S., Shahbazi, A., Wang, L., Wallace, C.W., 2010. Supercritical ethanol liquefaction of swine manure for bio-oils production. Am. J. Eng. Appl. Sci. 3, 494–500.